Progress In Electromagnetics Research, Vol. 123, 227–241, 2012

DEFORMABLE, TIME-VARYING BOUNDARY PROBLEMS IN ELECTRODYNAMICS

M. J. Mehler[1], C. C. Constantinou[1,*], and M. J. Neve[2]

[1]School of Electronic, Electrical & Computer Engineering, University of Birmingham, Edgbaston, Birmingham B15 2TT, UK

[2]Department of Electrical and Computer Engineering, University of Auckland, Private Bag 92019, Auckland, New Zealand

Abstract—A novel perturbation technique is formulated that enables the efficient calculation of current on surfaces undergoing time-varying mechanical deformations. The technique computes the current on the perturbed surface using as its starting point the solution for a related static case. This is initially derived using a standard analytical or numerical technique. The key advantage of this approach is that only an initial (computationally expensive) electromagnetic characterisation of the static problem is required. The surface current perturbation terms (and hence the radiated fields) are then directly computed from the static problem with a very low computational overhead.

1. INTRODUCTION

A broad class of engineering applications require the calculation of electromagnetic fields radiated or scattered by moving surfaces. For example, such problems commonly arise in radar applications where it is necessary to calculate the scattering cross-section and the spectral dispersion arising from moving targets. Often the profile of these targets is non-deterministic and the scattered fields are characterised using a statistical approach [1–3]. Typically, these authors exploit equivalent current methods and Physical Optics (PO) to determine the statistical properties of the scattered field. Moreover, these techniques can be used to treat representative targets such as planes, cylinders and spheres which are undergoing motions such as translation and vibration. In recent years much attention has also been given to

Received 20 October 2011, Accepted 16 December 2011, Scheduled 20 December 2011

* Corresponding author: Constantinos Constantinou (c.constantinou@bham.ac.uk).

scattering from deterministic surfaces undergoing translation, rotation and vibration. For example, one-dimensional deterministic scattering from vibrating planes [4, 5] and rotating cylinders [6] has been treated by applying relativistic boundary conditions and the method of characteristics to obtain numerical solutions.

In this paper, we consider the problem of scattering from surfaces undergoing mechanical processes that cause translation, rotation and deformation. These motions can be arbitrary, but are assumed to be described deterministically. Frequently these processes are time-harmonic in nature, as exemplified by vibrating panels on aircraft. The strict electromagnetic (EM) characterisation of such problems requires the solution of the wave equation subject to time-varying boundary conditions. Such rigorous solutions have only hitherto been attempted for the scalar wave equation (in one space dimension) to date [7] and are of limited applicability to practical problems. Moreover, obtaining a rigorous solution even when there is no time variation (i.e., for the static problem) is frequently very demanding. If approximations can be made (e.g., using high frequency asymptotic techniques such as the geometrical/uniform theories of diffraction) a considerable time saving can often be realised. However, approximate solutions to the full Boundary-Value Problem (BVP), e.g., Physical Optics (PO), are frequently needed in situations which cannot be solved exactly. An unfortunate characteristic of these 'full wave' solutions is that they are inevitably expensive to compute.

Sometimes geometries are so complex that even 'full-wave' solutions cannot be practically implemented. Fortunately, in recent times the challenge of modelling EM scattering from complex surfaces has been addressed by the development of versatile numerical methods, such as the Method of Moments (MoM) [8], and the Finite Difference Time Domain (FDTD) technique [9]. This requirement is further exacerbated if the problem being considered is time-varying, as computational runs must be repeated for a sequence of discrete snapshots — each of which represents an individual geometrical perturbation of the problem. As the computational load varies linearly with the number of geometrical perturbations to be considered, it can become prohibitively expensive, even for moderately sized problems where the boundary deformation is significant. Methods such as FDTD can be used more intelligently to accommodate moving boundaries using a general relativistic transformation [10], but still require significant processing resources to obtain results in acceptable timeframes.

The motivation for this paper is to develop a technique which can remove the requirement for performing a large number of independent

computational runs on geometries that — apart from relatively small-scale physical perturbations arising from mechanical translation, rotation and deformation — are otherwise identical. The approach presented here uses a novel perturbation technique to compute the current (or equivalent current) on a time-varying surface given knowledge of the current on an unperturbed (static) surface. The perturbation analysis adopted explicitly accounts for the effect of surface translation such that the remaining perturbation/correction terms need only account for the effect of surface deformation. The static problem can be computed via any appropriate analytical or numerical technique, so long as it is capable of producing a solution of acceptable accuracy for the static problem. A perturbation analysis is then used to estimate the variation in surface currents arising as a result of physical movement. In contrast to conventional perturbation theory [11, 12] the leading term in the expansion is not simply taken as being identical to the unperturbed case. The key feature of our approach is that only an initial (computationally expensive) EM characterisation of the static problem is required: The perturbation in surface currents (and hence the radiated fields) can be directly computed from the static problem using the technique presented here with a very low computational overhead.

The perturbation technique is formulated for an arbitrary perfectly conducting time varying surface, illuminated by a locally plane monochromatic wave. However, to demonstrate the efficacy of the technique, the induced surface current on a perfectly conducting circular cylinder, whose radius is varying harmonically, is calculated. This was chosen because the problem of scattering from a cylinder has been extensively studied in the literature [13–16] and a reliable analytic solution is easily obtained. The surface current distribution obtained via the perturbation analysis is compared with that obtained using repeated application of the analytical static solution technique calculated at every time step. Good agreement is observed, especially in the illuminated region, even for physical perturbations in excess of a wavelength.

2. PROBLEM FORMULATION

Consider the time-varying surface shown in Fig. 1, which supports a surface current $\mathbf{J}$. Following the usual conventions of differential geometry [17], the surface position vector $\mathbf{r}$ may be parameterised in terms of surface coordinates u, v. The effect of a time-varying surface deformation can then be introduced through the equation,

$$\mathbf{r}(u, v, t) = \mathbf{r}_0(u, v) + \boldsymbol{\delta}(u, v, t) \tag{1}$$

where $\mathbf{r}_0$ describes a static, unperturbed surface and $\boldsymbol{\delta}$ represents a time-varying perturbation. For this surface it is possible to determine an element of surface area dS in terms of the parameters u, v and a time varying Jacobian of the form,

$$dS = \xi(u, v, t) du dv \tag{2}$$

where $\xi(u, v, t) = \left| \frac{\partial \mathbf{r}}{\partial u} \times \frac{\partial \mathbf{r}}{\partial v} \right|$.

Similarly, with the aid of Eq. (1), the unit surface normal becomes,

$$\hat{\mathbf{n}} = \mathbf{n}_0 + \mathbf{n}_\delta \tag{3}$$

where $\mathbf{n}_0 = \left(\frac{\partial \mathbf{r}_0}{\partial u} \times \frac{\partial \mathbf{r}_0}{\partial v} \right) / \xi$ and $\mathbf{n}_\delta = \left(\frac{\partial \mathbf{r}_0}{\partial u} \times \frac{\partial \boldsymbol{\delta}}{\partial v} + \frac{\partial \boldsymbol{\delta}}{\partial u} \times \frac{\partial \mathbf{r}_0}{\partial v} + \frac{\partial \boldsymbol{\delta}}{\partial u} \times \frac{\partial \boldsymbol{\delta}}{\partial v} \right) / \xi$.

It also follows that,

$$\hat{\mathbf{n}} = \eta(u, v, t) \hat{\mathbf{n}}_0 + \mathbf{n}_\delta \tag{4}$$

where $\eta(u, v, t) = \left| \frac{\partial \mathbf{r}_0}{\partial u} \times \frac{\partial \mathbf{r}_0}{\partial v} \right| / \xi$, so that $\hat{\mathbf{n}}_0$ represents the unperturbed surface unit normal and $\mathbf{n}_\delta$ characterises the effect of the time-varying perturbation.

The field radiated by $\mathbf{J}$ can be found in the usual way by means of Green's theorem [18], where the free-space form of the Green's function is appropriate in this case. Strictly, for an arbitrary time-varying surface current, the full time-domain form of the Green's function should be used. However, a useful simplifying approximation can be made by observing that, surfaces varying at the rate of a few Hertz will appear almost static at a given instant in time from the point of view of the electromagnetic scattering process: In the time taken for the electromagnetic field to propagate across the scatterer, the latter

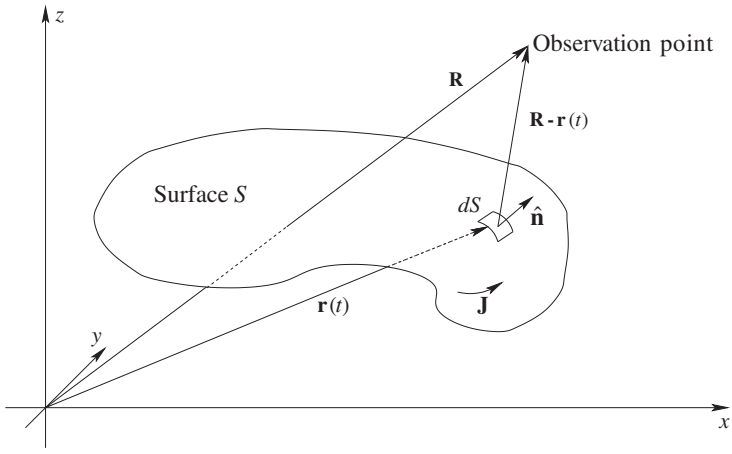

Figure 1. Geometry of time-varying surface.

will have moved only a negligibly small fraction of a wavelength. This can be exploited to simplify the form of the Green's function, which is thus taken to be of the steady-state form. Thus, provided that initial switching transients can be neglected, the field radiated by the surface current can be found quasi-statically using the time-harmonic form of the Green's function. Therefore, assuming $\mathbf{J}$ is excited by an incident monochromatic plane wave, the scattered field is given by,

$$\mathbf{A}(\mathbf{R},t) = \mu_0 \int_S \mathbf{J}(\mathbf{R},t) G(\mathbf{R},\mathbf{r}) \xi(u,v,t) du dv \tag{5}$$

where $G(\mathbf{R},\mathbf{r}) = \frac{e^{-jk|\mathbf{R}-\mathbf{r}|}}{4\pi|\mathbf{R}-\mathbf{r}|}$; with reference to Fig. 1, $\mathbf{R}$ is the position vector of the observation point, $\mathbf{r}$ is the source coordinate over which the integration is taken and is a function of u, v and t, as defined by Eq. (1).

The aim here is to derive an expression for the induced surface current $\mathbf{J}$, subject to the time-varying boundary perturbation described by Eq. (1), given that the unperturbed current on $\mathbf{r}_0$ is known. It is assumed that this unperturbed current $\mathbf{J}_0$ on S has been calculated using an analytical solution where this exists, or via an appropriate numerical technique. To determine the relationship between $\mathbf{J}$ and $\mathbf{J}_0$ it is necessary to consider the associated BVP. Assuming a perfectly conducting surface S is illuminated by an incident plane wave $\mathbf{E}^i$, a surface current $\mathbf{J}$ will be induced which radiates a scattered field $\mathbf{E}^s$, satisfying the condition,

$$\hat{\mathbf{n}} \times \left(\mathbf{E}^i + \mathbf{E}^s\right) = 0 \text{ on } S. \tag{6}$$

Since $\hat{\mathbf{n}}$ is the surface normal, this merely expresses the constraint that the tangential component of $\mathbf{E}$ vanishes. The electric field radiated by $\mathbf{J}$ can be obtained from Eq. (5) by application of Maxwell's equations, in the form [19],

$$\mathbf{E}(\mathbf{R},t) = -j \int_S \left(\omega\mu_0 + \frac{\boldsymbol{\nabla}\boldsymbol{\nabla}\cdot}{\omega\epsilon_0}\right) \mathbf{J}(\mathbf{R},t) G(\mathbf{R},\mathbf{r}) \xi du dv \tag{7}$$

and for convenience in later analysis this can be represented in a linear operator notation as,

$$\mathbf{E}(\mathbf{R},t) = \mathcal{L}_S\left[\mathbf{J};\mathbf{R}\right] \tag{8}$$

where the subscript S denotes the surface over which the integration implied by $\mathcal{L}$ is taken.

Using the above notation it is possible to express the BVP concisely. Considering initially the unperturbed case, where $\mathbf{r} = \mathbf{r}_0$, then $\mathbf{J}_0$ satisfies,

$$\hat{\mathbf{n}}_0 \times \left(\mathbf{E}^i\left(\mathbf{r}_0(u,v)\right) + \mathcal{L}_S\left[\mathbf{J}_0;\mathbf{r}_0(u,v)\right]\right) = 0 \tag{9}$$

for $u, v \in D$ and where $\mathbf{E}^i(\mathbf{r}_0) = \mathbf{E}_0 \exp(-j\mathbf{k}_0.\mathbf{r}_0)$.

It should be noted that, in Eq. (9), the observation point is now coincident with the surface $\mathbf{r}_0$, and the parameters u, v vary over the integration domain D in order to generate the surface S. If the surface now undergoes the perturbation described by Eq. (1), $\mathbf{r} = \mathbf{r}_0 + \boldsymbol{\delta}$, then $\hat{\mathbf{n}} = \mathbf{n}_0 + \mathbf{n}_\delta$ and $S \to S'$. The resulting BVP now becomes,

$$(\mathbf{n}_0 + \mathbf{n}_\delta) \times \left(\mathbf{E}^i(\mathbf{r}(u,v,t)) + \mathcal{L}_{S'}[\mathbf{J}; \mathbf{r}(u,v,t)]\right) = 0 \tag{10}$$

for $u, v \in D$. To proceed it is now necessary to express $\mathbf{J}$ in terms of the unperturbed current $\mathbf{J}_0$ and a series of perturbation terms. The magnitude of these perturbation terms compared to $\mathbf{J}_0$ can be significantly reduced, and the method made more computationally efficient, by recognising that the bulk effect of deforming the surface will be to induce a phase shift proportional to the distance moved in the direction of the incident wave, together with a small change in surface area. These effects can then be explicitly included in the leading term of the expansion, resulting in an expression of the form,

$$\mathbf{J} = e^{-j\mathbf{k}_0.\boldsymbol{\delta}} \eta \mathbf{J}_0 + \mathbf{J}_1 + \mathbf{J}_2 \tag{11}$$

where two perturbation terms $\mathbf{J}_1$ and $\mathbf{J}_2$ have been included, rather than a single term, because they can be made to satisfy separable equations. To this end, $\mathbf{J}_1$ is defined so that it satisfies,

$$\mathcal{L}_{S'}[\mathbf{J}_1; \mathbf{r}] = e^{-j\mathbf{k}_0.\boldsymbol{\delta}} \mathcal{L}_S[\mathbf{J}_0; \mathbf{r}_0] - \mathcal{L}_{S'}\left[e^{-j\mathbf{k}_0.\boldsymbol{\delta}} \eta \mathbf{J}_0; \mathbf{r}\right] \tag{12}$$

for $u, v \in D$, so that combining Eq. (10) with the expansion of Eq. (11) and eliminating the term operated upon by $\mathcal{L}_{S'}$ using Eq. (12), yields,

$$\begin{aligned} &\mathbf{n}_0 \times \left(\mathbf{E}^i(\mathbf{r}) + e^{-j\mathbf{k}_0.\boldsymbol{\delta}} \mathcal{L}_S[\mathbf{J}_0; \mathbf{r}_0]\right) + \mathbf{n}_0 \times \mathcal{L}_{S'}[\mathbf{J}_2; \mathbf{r}] \\ &+ \mathbf{n}_\delta \times \left\{\mathbf{E}^i(\mathbf{r}) + e^{-j\mathbf{k}_0.\boldsymbol{\delta}} \mathcal{L}_S[\mathbf{J}_0; \mathbf{r}_0] + \mathcal{L}_{S'}[\mathbf{J}_2; \mathbf{r}]\right\} = 0 \end{aligned} \tag{13}$$

for $u, v \in D$. Making use of Eq. (9), together with $\mathbf{E}^i(\mathbf{r}) = \mathbf{E}^i(\mathbf{r}_0) e^{-j\mathbf{k}_0.\boldsymbol{\delta}}$, shows that the above choice of $\mathbf{J}_1$ ensures the first bracketed term vanishes and $\mathbf{J}_2$ satisfies,

$$\hat{\mathbf{n}} \times \mathcal{L}_{S'}[\mathbf{J}_2; \mathbf{r}] = -\mathbf{n}_\delta \times \left\{\mathbf{E}^i(\mathbf{r}) + e^{-j\mathbf{k}_0.\boldsymbol{\delta}} \mathcal{L}_S[\mathbf{J}_0; \mathbf{r}_0]\right\} \tag{14}$$

for $u, v \in D$.

In effect the original BVP expressed by Eq. (10) has been replaced by Eqs. (12) and (14) for the perturbation currents $\mathbf{J}_1$ and $\mathbf{J}_2$, respectively. Moreover, it can be seen that the right hand side of Eq. (12) depends on the difference between two similar terms and the right hand side of Eq. (14) is proportional to the small perturbation

vector $\mathbf{n}_\delta$. Thus it is to be expected that the perturbation terms $\mathbf{J}_1$ and $\mathbf{J}_2$ will be of the order of the perturbation and hence small compared to the leading term in Eq. (11). In fact, the effects of surface translations are explicitly included in the leading term of Eq. (11) and make no contribution to the remaining terms. To make this explicit, consider the special case when the surface undergoes a time dependent translation, without deformation. This is described by, $\mathbf{r}(u,v,t) = \mathbf{r}_0(u,v) + \boldsymbol{\delta}(t)$, where $\boldsymbol{\delta}$ is expressly not a function of u, v. Since the Green's function in Eq. (7) has an argument which depends on the difference between the source and observation coordinates, such a translation leaves its value unchanged. This observation, together with the definition of η given by Eq. (4), applied to Eqs. (7) and (8), yields,

$$\mathcal{L}_{S'}\left[e^{-j\mathbf{k}_0\cdot\boldsymbol{\delta}}\eta\mathbf{J}_0;\mathbf{r}\right] = e^{-j\mathbf{k}_0\cdot\boldsymbol{\delta}}\mathcal{L}_S\left[\mathbf{J}_0;\mathbf{r}_0\right]. \tag{15}$$

Thus it is possible to conclude that the right hand side of Eq. (12) vanishes and $\mathbf{J}_1 = 0$. Moreover, from Eq. (3) it is evident that $\mathbf{n}_\delta = 0$ and thus the right hand side of Eq. (14) vanishes, consequently resulting in $\mathbf{J}_2 = 0$. Therefore, for the special case of translation without surface deformation, it can be inferred that $\mathbf{J}_1 = \mathbf{J}_2 = 0$, and the first term of Eq. (11) is an exact solution. In the presence of a surface deformation, which introduces a non-zero $\mathbf{n}_\delta$, the perturbation terms $\mathbf{J}_1$ and $\mathbf{J}_2$ are non-zero.

Unfortunately, the rigorous determination of $\mathbf{J}_1$ and $\mathbf{J}_2$ by the solution of Eqs. (12) and (14) is a procedure equal in complexity to solving the original BVP, given by Eq. (10). However, it is possible to simplify this procedure by exploiting PO [19] to approximate $\mathbf{J}_1 + \mathbf{J}_2$. The PO approximation determines the surface current in terms of the incident magnetic field $\mathbf{H}^i$, through the relation $\mathbf{J}_{\mathrm{PO}} = 2\hat{\mathbf{n}} \times \mathbf{H}^i$. Therefore, the perturbed PO current may be written as,

$$\mathbf{J}_{\mathrm{PO}} = 2\left(\mathbf{n}_0 + \mathbf{n}_\delta\right) \times \mathbf{H}_0 e^{-j\mathbf{k}_0\cdot\mathbf{r}} \tag{16}$$

where use has been made of Eq. (3) and $\mathbf{H}^i = \mathbf{H}_0 e^{-j\mathbf{k}_0\cdot\mathbf{r}}$ is the incident magnetic field. This can be further expanded by means of Eqs. (1) and (4), to yield,

$$\mathbf{J}_{\mathrm{PO}} = e^{-j\mathbf{k}_0\cdot\boldsymbol{\delta}}\eta\mathbf{J}_0' + 2\mathbf{n}_\delta \times \mathbf{H}_0 e^{-j\mathbf{k}_0\cdot\mathbf{r}} \tag{17}$$

where $\mathbf{J}_0' = 2\hat{\mathbf{n}}_0 \times \mathbf{H}_0 e^{-j\mathbf{k}_0\cdot\mathbf{r}_0}$.

Here $\mathbf{J}_0'$ is the unperturbed current on $\mathbf{r}_0$ determined to within the PO approximation, unlike $\mathbf{J}_0$ which is exact. Eq. (17) can be used to approximate $\mathbf{J}_1 + \mathbf{J}_2$, by direct comparison with Eq. (11),

$$\mathbf{J}_1 + \mathbf{J}_2 \approx 2\mathbf{n}_\delta \times \mathbf{H}_0 e^{-j\mathbf{k}_0\cdot\mathbf{r}}. \tag{18}$$

Finally, incorporating this result into Eq. (11), yields,

$$\mathbf{J} \approx e^{-j\mathbf{k}_0.\boldsymbol{\delta}}\eta\mathbf{J}_0 + 2\mathbf{n}_\delta \times \mathbf{H}_0 e^{-j\mathbf{k}_0.\mathbf{r}}. \tag{19}$$

Whilst the first term in this equation is exact, the second term is subject to the PO approximation. Hence the approximation will deteriorate if the dimensions of the scatterer are electrically small. In practice, this means the method becomes unreliable for scatterers of a few wavelengths extent, with small radii of curvature and significant edge effects [19]. Fortunately, these cases can be tackled efficiently using numerical methods without the need to resort to perturbation techniques.

It is also instructive to derive the far-field radiated by the surface current, given by Eq. (19). This is straightforward to derive from Eq. (5) by making use of the usual far-field approximation $|\mathbf{R} - \mathbf{r}| \sim R - \mathbf{r}.\hat{\mathbf{R}}$, which yields,

$$\mathbf{A} \sim \frac{\mu_0}{4\pi}\frac{e^{-jkR}}{R}\int_S \mathbf{J}e^{jk(\hat{\mathbf{R}}.\mathbf{r})}\xi du dv. \tag{20}$$

Substituting Eq. (19) into Eq. (20) and making use of Eqs. (1)–(4), gives,

$$\begin{aligned}\mathbf{A} = \frac{\mu_0}{4\pi}\frac{e^{-jkR}}{R}\int_S \Bigg\{ & \mathbf{W}(u,v)e^{jk((\hat{\mathbf{R}}-\hat{\mathbf{k}}_0).\boldsymbol{\delta})} \\ & +2\left(\frac{\partial \mathbf{r}_0}{\partial u}\times\frac{\partial \boldsymbol{\delta}}{\partial v}+\frac{\partial \boldsymbol{\delta}}{\partial u}\times\frac{\partial \mathbf{r}_0}{\partial v}+\frac{\partial \boldsymbol{\delta}}{\partial u}\times\frac{\partial \boldsymbol{\delta}}{\partial v}\right)\times\mathbf{H}_0 e^{jk((\hat{\mathbf{R}}-\hat{\mathbf{k}}_0).\mathbf{r})}\Bigg\} du dv\end{aligned} \tag{21}$$

where,

$$\mathbf{W}(u,v) = \mathbf{J}_0 e^{jk(\hat{\mathbf{R}}.\mathbf{r}_0)}\left|\frac{\partial \mathbf{r}_0}{\partial u}\times\frac{\partial \mathbf{r}_0}{\partial v}\right|. \tag{22}$$

It is evident from Eq. (20) that $\mathbf{W}$ is just the integrand associated with the unperturbed case ($\boldsymbol{\delta} = 0$). Therefore, it is possible to conclude from Eq. (21) that effect of the perturbation is to introduce an additional phase factor $e^{jk((\hat{\mathbf{R}}-\hat{\mathbf{k}}_0).\boldsymbol{\delta})}$, and a perturbation term proportional to the first order derivatives of $\boldsymbol{\delta}$. As the extent of the perturbation is increased, this phase factor will reduce the coherence of $\mathbf{W}$ and hence the significance of the first term compared with the second. The second term which arises solely because of the perturbation, is proportional to the degree of surface deformation, as characterised by $\frac{\partial \boldsymbol{\delta}}{\partial u}$ and $\frac{\partial \boldsymbol{\delta}}{\partial v}$. It should also be remarked that since $\boldsymbol{\delta}$ is a function of t, the scattered field will also undergo spectral dispersion. In practice this effect will be small since the rate of surface deformation is small compared with the frequency of the incident field.

Nevertheless, this effect can be quantified by explicitly computing the electric field in the time domain using, $\mathbf{E} = \frac{\partial}{\partial t}(\Re(e^{j\omega t}\mathbf{A}))$.

In the next section the range of validity of Eq. (19) is investigated by comparison with the canonical solution for a right circular cylinder.

3. COMPARISON OF PERTURBATION METHOD WITH CANONICAL CYLINDER SOLUTION

To investigate the accuracy of Eq. (19), it can be compared directly with the canonical solution for a right circular perfectly conducting cylinder over a range of parameter values. Fig. 2 illustrates a perfectly conducting circular infinite cylinder, with its axis along the $\hat{\mathbf{z}}$-direction. It is illuminated by a homogeneous uniform plane wave of unit field strength propagating in the $\hat{\mathbf{x}}$-direction. The cylinder has a radius a_0 and the incident field is assumed to be magnetically polarised with $\mathbf{H}^i$ along the $\hat{\mathbf{z}}$-direction. By imposing the boundary condition $E_\theta = 0$ on the surface of the cylinder, a solution for the total magnetic field H_z can be obtained in terms of a series of cylindrical modes [13], namely,

$$H_z = \sum_{n=-\infty}^{\infty} \frac{j^{-n}e^{jn\theta}}{H_n^{(2)\prime}(k_0a_0)} \times \left\{ J_n(k_0a_0)H_n^{(2)\prime}(k_0a_0) - J_n'(k_0a_0)H_n^{(2)}(k_0a_0) \right\}. \quad (23)$$

The associated surface current is given by $\mathbf{J} = \hat{\mathbf{n}} \times \mathbf{H}$, which in this case reduces to the azimuthal current $J_\theta = -H_z$.

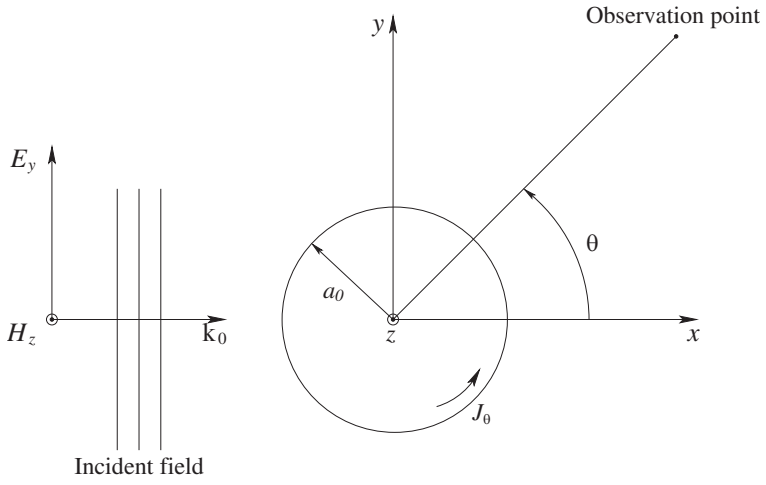

Figure 2. Geometry of canonical cylinder problem.

Now consider the case when the cylinder's radius is time-varying, so that in the notation of Eq. (1),

$$\begin{aligned} \mathbf{r}_0 &= (a_0 \cos u, a_0 \sin u, v) \qquad \text{and} \\ \boldsymbol{\delta} &= (\Delta \sin \omega_s t \cos u, \Delta \sin \omega_s t \sin u, 0). \end{aligned} \tag{24}$$

This implies that the radius is varying sinusoidally about a_0 by $\pm\Delta$. The angular frequency of this motion, ω_s, which is assumed mechanical in origin, is orders of magnitude less than the radio frequency ω. Hence an exact solution can be obtained from Eq. (23), since the displacement is quasi-static, by replacing $a_0 \to a_0 + \Delta \sin \omega_s t$. Furthermore, Eqs. (3) and (4) lead to the results,

$$\mathbf{n}_\delta = \frac{\Delta \sin \omega_s t}{a_0 + \Delta \sin \omega_s t}(\cos u, \sin u, 0) \qquad \eta = \frac{a_0}{a_0 + \Delta \sin \omega_s t}. \tag{25}$$

Since the incident plane wave is $\hat{\mathbf{x}}$-directed, $\mathbf{k}_0 = \frac{2\pi}{\lambda_0}\hat{\mathbf{x}}$ and hence,

$$\mathbf{k}_0 \cdot \boldsymbol{\delta} = \frac{2\pi\Delta}{\lambda_0} \sin \omega_s t \cos u \qquad \mathbf{k}_0 \cdot \mathbf{r} = \frac{2\pi}{\lambda_0}(a_0 + \Delta \sin \omega_s t) \cos u. \tag{26}$$

Substituting Eqs. (24)–(26) in Eq. (19) and noting that in this example $u \equiv \theta$, yields,

$$J_\theta = \frac{-e^{-jk_0 \Delta \sin \omega_s t \cos \theta}}{a_0 + \Delta \sin \omega_s t} \times \left\{ a_0 J_0 + 2\Delta \sin \omega_s t e^{-jk_0 a \cos \theta} U\left(\theta - \frac{\pi}{2}\right) \right\}. \tag{27}$$

Here J_0 is the unperturbed ($\boldsymbol{\delta} = 0$) azimuthal component of current derived from Eq. (23). $U(x)$ is a unit step function and is included because the PO current is only non-zero in the illuminated region $\frac{\pi}{2} \leq \theta \leq \pi$.

Figures 3 and 4 show comparisons between the magnitude of the azimuthal current J_θ calculated using the exact solution given by Eq. (23) and the perturbation method described by Eq. (27). Since the perturbation is at a maximum when $\sin \omega_s t = \pm 1$, which corresponds to the most extreme surface deformation $a_0 \to a_0 \pm \Delta$, these figures illustrate this instance. Fig. 3 show the cases $a_0 = 3\lambda_0$ with $\Delta = \pm 0.5\lambda_0, \pm\lambda_0$, whereas Fig. 4 plot results for $a_0 = 9\lambda_0$ with $\Delta = \pm\lambda_0, \pm 2\lambda_0$. As might be anticipated, these plots show that exact and perturbation methods begin to diverge as Δ increases. Nevertheless, the perturbation method remains good out to quite large values of Δ. Specifically, for the $3\lambda_0$ radius cylinder, $\Delta = \lambda_0$ ($0.33a_0$) and for the $9\lambda_0$ radius cylinder $\Delta = 2\lambda_0$ ($0.22a_0$). In all cases agreement in the illuminated region $90^\circ \leq \theta \leq 180^\circ$ is excellent, where the computed values show differences of < 0.1 dB. This also applies to the differences in phase which were computed to be $< 3^\circ$.

In the shadow region $0 \leq \theta < 90°$, where the perturbation terms $\mathbf{J}_1$ and $\mathbf{J}_2$ are taken as zero, differences begin to appear as Δ increases. Although agreement between magnitudes is still quite good over the whole range, in the shadow region for large perturbations ($a = 9\lambda$, $\Delta = 2\lambda$), below about -20 dB, phase errors of around 50° are possible. Moreover, in the deep shadow region $0 \leq \theta < 45°$, especially near pattern nulls where the phase is very oscillatory, its estimate can become unreliable. However, this is an extreme test, since prediction in the shadow region at these levels is notoriously difficult even with analytic solution techniques. Fortunately, the contribution to the radiation integral, Eq. (20), is mostly from the dominant current in the illuminated region and the scattered field derived will be little affected by errors in these exceedingly small shadow region currents. This turns out to be particularly the case along the principal scattering directions.

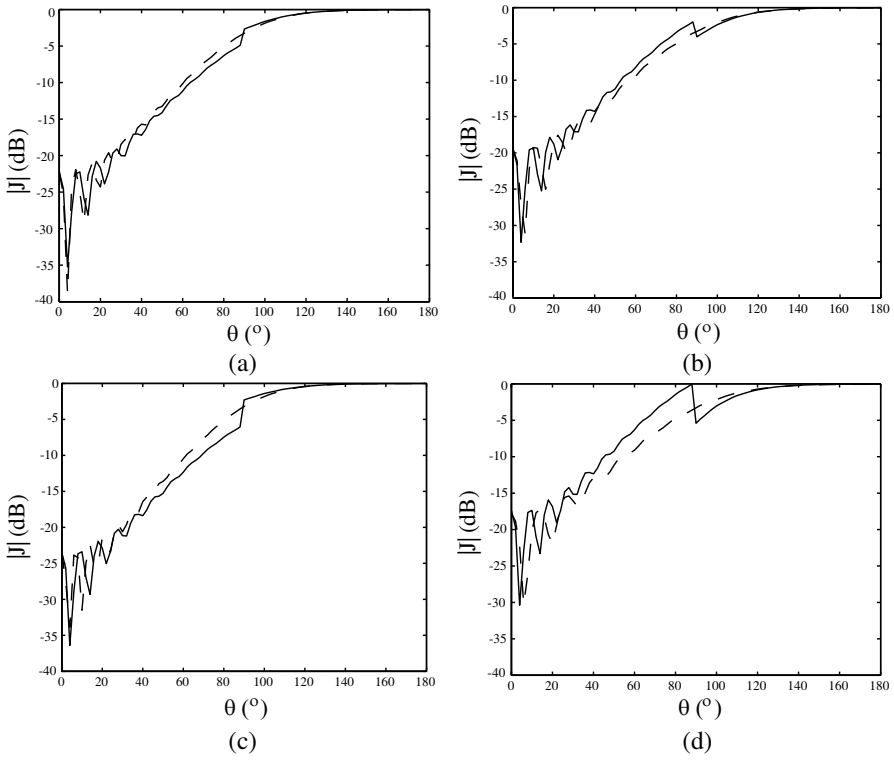

Figure 3. Time-varying cylinder with instantaneous radius $3\lambda_0 + \Delta$. The solid line represents the solution using the proposed perturbation method, whereas the dashed line represents the 'exact' series solution. (a) $\Delta = 0.5\lambda_0$. (b) $\Delta = -0.5\lambda_0$. (c) $\Delta = \lambda_0$. (d) $\Delta = -\lambda_0$.

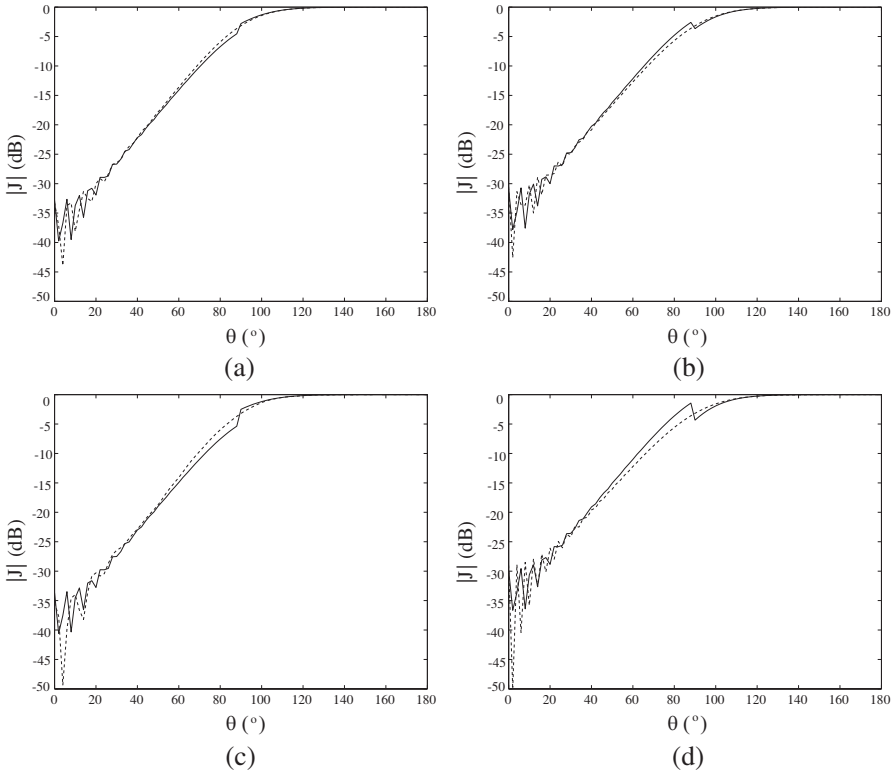

Figure 4. Time-varying cylinder with instantaneous radius $9\lambda_0 + \Delta$. The solid line represents the solution using the proposed perturbation method, whereas the dashed line represents the 'exact' series solution. (a) $\Delta = \lambda_0$. (b) $\Delta = -\lambda_0$. (c) $\Delta = 2\lambda_0$. (d) $\Delta = -2\lambda_0$.

Furthermore, it follows directly from Eq. (27), that the relative magnitude of the perturbation term $\mathbf{J}_1 + \mathbf{J}_2$, compared with the leading term in Eq. (11), varies linearly with Δ as $2\Delta/(a_0|\mathbf{J}_0|)$. The significance of these two correction terms is illustrated numerically in Fig. 5. As is clearly evident in the results, the significance of the PO approximation becomes more important as the degree of perturbation increases. Moreover, Figs. 3 and 4 show that the accuracy of the method tends to improve as the radius of curvature increases. This is consistent with the behaviour of the PO approximation which improves in accuracy as the surface becomes more planar.

It is of interest to increase Δ to the point where the method completely breaks down. Fig. 6 illustrates this situation for $a_0 = 3\lambda_0$ and $\Delta = 3\lambda_0, -2\lambda_0$. At this point the perturbation method gives

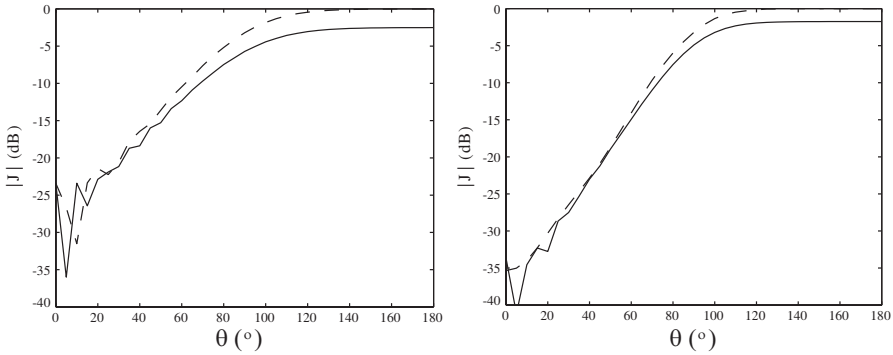

Figure 5. The effect of "switching off" the perturbation correction terms $\mathbf{J}_1 + \mathbf{J}_2$. The solid line represents the leading term in the perturbation solution alone, whereas the dashed line represents the full perturbation solution. (a) $a_0 = 3\lambda_0$ and $\Delta = \lambda_0$. (b) $a_0 = 9\lambda_0$ and $\Delta = 2\lambda_0$.

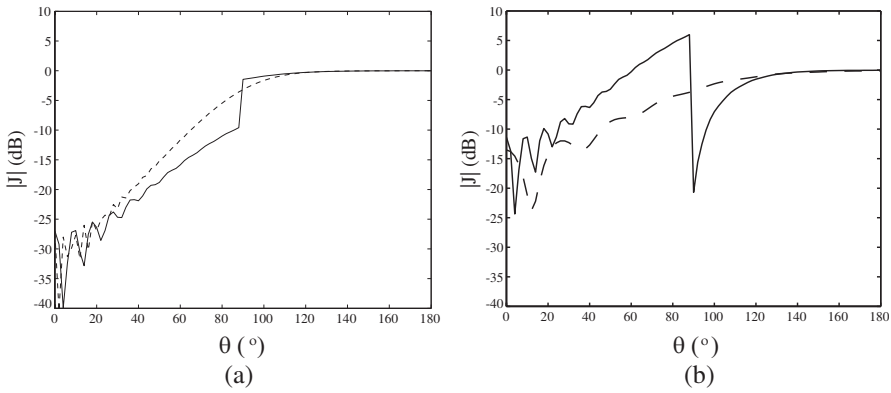

Figure 6. Time-varying cylinder with instantaneous radius $3\lambda_0 + \Delta$. The solid line represents the solution using the proposed perturbation method, whereas the dashed line represents the 'exact' series solution. (a) $\Delta = 3\lambda_0$. (b) $\Delta = -2\lambda_0$.

poor results, even in the illuminated region. However, this is an extreme example, since at this point the radius has undergone a 100% increase or 66% decrease. In the latter case the PO approximation has completely broken down for a cylinder of radius λ_0. In general it may be concluded that the technique is reliable out to radius of curvature changes of $\sim 20\%$. Beyond this point, shadow region predictions start to become unreliable. It should also be remarked that the canonical solution given by Eq. (23) is very slow to converge, requiring 78

summation terms for the $9\lambda_0$ radius cylinder. In contrast, once $\mathbf{J}_0$ is determined, Eq. (27) is trivial to compute.

4. CONCLUSION

A novel perturbation technique is formulated that enables the efficient calculation of current on surfaces undergoing time varying mechanical deformations. The technique computes the current on the time varying surface using as its starting point the solution for a related static case, which is derived using a standard analytical or numerical technique. The approach is made more computationally efficient by explicitly accounting for the effect of surface translation so that the remaining perturbation/correction terms need only account for the effect of surface deformation. Moreover, only an initial computationally expensive EM characterisation of the static problem is required. The perturbation in surface currents (and hence the radiated fields) is then directly computed from the static problem with a very low computational overhead.

The efficacy of the technique is demonstrated by computing the induced surface current on a perfectly conducting circular cylinder, whose radius is varying harmonically. The surface current distribution obtained via the perturbation analysis is compared with that obtained using repeated application of the analytical static solution technique. Good agreement is observed both in terms of amplitude and phase, especially in the illuminated region, even for physical perturbations in excess of a wavelength.

REFERENCES

1. Abdelazeez, M., L. Peach, and S. Borkar, "Scattering of electromagnetic waves from moving surfaces," *IEEE Trans. Antennas Propagat.*, Vol. 27, No. 5, 679–684, 1979.
2. Kleinman, R. and R. Mack, "Scattering by linearly vibrating objects," *IEEE Trans. Antennas Propagat.*, Vol. 27, No. 3, 344–352, 1979.
3. Van Bladel, J. and D. De Zutter, "Reflections from linearly vibrating objects: Plane mirror at normal incidence," *IEEE Trans. Antennas Propagat.*, Vol. 29, No. 4, 629–637, 1981.
4. Ho, M., "One-dimensional simulation of reflected EM pulses from objects vibrating at different frequencies," *Progress In Electromagnetics Research*, Vol. 53, 239–248, 2005.
5. Ho, M., "Numerical simulation of scattering of electromagnetic waves from traveling and/or vibrating perfect conducting planes," *IEEE Trans. Antennas Propagat.*, Vol. 54, No. 1, 152–156, 2006.

6. Ho, M., "Simulation of scattered em fields from rotating cylinder using passing center swing back grids technique in two dimensions," *Progress In Electromagnetics Research*, Vol. 92, 79–90, 2009.
7. Pelloni, B. and D. A. Pinotsis, "Moving boundary value problems for the wave equation," *Journal of Comp. and Appl. Math.*, Vol. 234, 1685–1691, 2010.
8. Harrington, R. F., *Field Computation by Moment Methods*, Wiley, 1993.
9. Taflove, A. and S. C. Hagness, *Computational Electrodynamics: The Finite-difference Time-domain Method*, Artech House, Boston, 2005.
10. Armenta, R. B. and C. D. Sarris, "Exploiting the relativistic formulation of maxwells equations to introduce moving grids into finite difference time domain solvers," *Proc. IEEE Intl. Microw. Symp. (MTT-S)*, 93–96, 2010.
11. Marcuse, D., *Theory of Dielectric Optical Waveguides*, Academic Press, 1991.
12. Johnson, S. G., M. Ibanescu, M. A. Skorobogatiy, O. Weisberg, J. D. Joannopoulos, and Y. Fink, "Perturbation theory for maxwells equations with shifting material boundaries," *Phys. Rev. E*, Vol. 65, 066611, 2002.
13. Wait, J. R., *Introduction to Antennas and Propagation*, Peregrinus, London, 1986.
14. Ahmed, S. and Q. A. Naqvi, "Electromagnetic scattering from a perfect electromagnetic conductor cylinder buried in a dielectric half-space," *Progress In Electromagnetics Research*, Vol. 78, 25–38, 2008.
15. Henin, B. H., A. Z. Elsherbeni, and M. H. Al Sharkawy, "Oblique incidence plane wave scattering from an array of circular dielectric cylinders," *Progress In Electromagnetics Research*, Vol. 68, 261–279, 2007.
16. Yan, W.-Z., Y. Du, Z. Li, E.-X. Chen, and J.-C. Shi, "Characterization of the validity region of the extended T-matrix method for scattering from dielectric cylinders with finite length," *Progress In Electromagnetics Research*, Vol. 96, 309–328, 2009.
17. Kreyszig, E., *Differential Geometry*, Dover, New York, 1991.
18. Jackson, J. D., *Classical Electrodynamics*, Wiley, New York, 1975.
19. Balanis, C. A., *Advanced Engineering Electromagnetics*, Wiley, New York, 1989.